Quantum bound states around black holes

J. Grain[a], A. Barrau[b]

Laboratoire de Physique Subatomique et de Cosmologie de Grenoble, UJF-CNRS-IN2P3-INPG, 53 avenue des Martyrs, 38026 Grenoble cedex, France

Abstract. Quantum mechanics in the vicinity of black holes is a fascinating field of theoretical physics. It involves both general relativity and particle physics, opening new eras to establish the principles of unified theories. In this article, we show that quantum bound states with no classical equivalent – as can easily be seen at the dominant monopolar order – should be formed around black holes for massive scalar particles. We qualitatively investigate some important physical consequences, in particular for the Hawking evaporation mechanism and the associated greybody factors.

PACS. 04.62.+v; 04.70.Dy; 04.70-s

1 Introduction

Black holes are extreme objects whose study is very rich and relies on different branches of physics. Among the most important and fundamental phenomena of black hole physics are the Hawking evaporation mechanism – see [1] for a review – and the existence of quasi-normal modes (QNMs) – see [2] for a review. On the one hand, the evaporation phenomenon reveals the profound links between gravity and thermodynamics. Its study is both extremely fruitful in itself and because of the quantum gravitational effects expected to occur during the last stages of the evaporation, when the semi-classical approach breaks down. On the other hand, quasi-normal modes are of particular importance because they revealed black holes to be stable under perturbations and represent a key ingredient in the computation of gravitational wave signals.

This article focuses on the investigation of bound states for massive particles emitted by black holes. The problem is mathematically quite close to the investigation of massive QNMs [3], as in both cases the point is to find the characteristic complex frequencies allowing a massive (scalar) field to propagate in a black hole background, while satisfying given boundary conditions at the black hole horizon and at spatial infinity (see, e.g., [4]). Nevertheless because those boundary conditions are not the same, the physical meaning of bound states and quasi-normal modes are very different and correspond to different energy ranges. Although bound states are well known to exist in quite a lot of classical and quantum systems, this work

points out their specific existence around black holes, even at the monopolar order, and investigates some important consequences. In most of the literature, bound states refer both to particles *orbiting* the black hole or back scattered to the black hole. In this work, we are interested in quanta trapped between the finite black hole potential barrier and the infinitely thick well which prevents the particles from reaching infinity if their energy is low enough. As will be demonstrated hereafter, those orbiting states are not strictly stable but can be characterized by finite lifetimes.

In Sect. 2, we first determine the conditions for such states to exist and compute their energy spectra and lifetimes at the WKB order. Thanks to a simple toy model, we can estimate in Sect. 3 the average number of trapped particles as a function of their characteristic energies. Those trapped massive particles – whose greybody factors must be computed numerically – will also inevitably modify the Hawking radiation spectrum at infinity, which is computed in this section. Some conclusions are finally given together with perspectives.

2 Orbiting bound states

The investigation of orbiting quantum bound states around Schwarzschild black holes requires one to solve relativistic quantum mechanical equations in a curved background, while taking into account a non-vanishing mass. To show that those states do exist, the Klein–Gordon equation in a Schwarzschild background will be shown to exhibit a radial potential containing a local well for given ranges of black hole horizon radii and particle masses.

[a] e-mail: grain@apc.univ-paris7.fr
[b] e-mail: barrau@in2p3.fr

2.1 Conditions for such states

The Klein–Gordon equation of motion for a scalar field Φ with mass μ in a space-time with metric $g_{\alpha\beta}$ can be expressed as

$$\frac{1}{\sqrt{-g}}\partial_\alpha\left(\sqrt{-g}\,g^{\alpha\beta}\partial_\beta\Phi\right)+\mu^2\Phi=0\,. \tag{1}$$

Writing $\Phi=\mathrm{e}^{-\mathrm{i}\omega t}Y_m^\ell(\theta,\varphi)R(r)$ to split the temporal, angular and radial parts of the field (where Y_m^ℓ are the spherical harmonics), the radial function $R(r)$ obeys, in a 4-dimensional Schwarzschild background,

$$\left[\frac{h(r)}{r^2}\frac{\mathrm{d}}{\mathrm{d}r}h(r)r^2\frac{\mathrm{d}}{\mathrm{d}r}+\omega^2-h(r)\left(\frac{\ell(\ell+1)}{r^2}+\mu^2\right)\right]R(r)=0\,, \tag{2}$$

where $h(r)$ is defined by the metric $\mathrm{d}s^2=h(r)\mathrm{d}t^2-\mathrm{d}r^2/h(r)-r^2\mathrm{d}\Omega^2$ (see, e.g., [5] and references therein for a description of the general techniques associated with quantum fields in a Schwarzschild spacetime used throughout this paper). Under the change of variables $r\to r_*$ and $R(r)\to U(r)$ where r_* is the tortoise coordinate (such that $\mathrm{d}r_*=\mathrm{d}r/h(r)$) and $U(r)=rR(r)$, this equation takes a Schrödinger-like form

$$\frac{\mathrm{d}^2U}{\mathrm{d}r_\star^2}+\left(\omega^2-V_\ell^2(r)\right)U=0\,, \tag{3}$$

with a potential

$$V_\ell^2(r)=\left(1-\frac{r_H}{r}\right)\left(\frac{\ell(\ell+1)}{r^2}+\frac{r_H}{r^3}+\mu^2\right)\,, \tag{4}$$

where r_H stands for the Schwarzschild radius and ℓ for the angular quantum number. The usual quantum mechanical techniques can therefore be employed in the tortoise coordinate system. The Chandrasekhar convention is
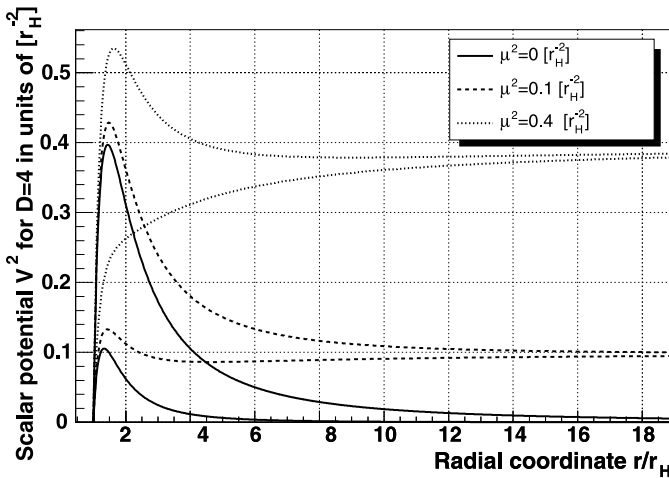

Fig. 1. Square of the potential as a function of the radial coordinate for three values of the mass μ and two values of the angular quantum number ℓ (in each case, $\ell=0$ for the *lower curve* and $\ell=1$ for the *upper curve*)

used hereafter: the last term of (3) is interpreted as the squared potential so as to recover the standard Hamilton–Jacobi equation. On Fig. 1, $V_\ell^2(r)$ is shown for three different values of the mass ($\mu=\{0,\sqrt{0.1},\sqrt{0.4}\}\,[r_H^{-1}]$) and two values of the angular momentum ($\ell=0$ and $\ell=1$). Depending on μ and ℓ, it can be seen that a local minimum, potentially leading to a bound state, eventually appears. The existence of a potential well depends on the roots of the algebraic equation $\frac{\mathrm{d}V_\ell^2}{\mathrm{d}r}=0$:

$$r_H\mu^2r^3-2\ell(\ell+1)r^2-3r_H(1-\ell(\ell+1))r+4r_H^2=0\,. \tag{5}$$

Two roots above r_H exist if the mass μ is lower than a critical value $\mu_+(\ell)$ given by

$$\mu_+^2=\frac{1}{216r_H^2}\left(-27J_1+\sqrt{729J_1^2+432J_2}\right)\,, \tag{6}$$

with

$$J_1=\ell^3(\ell+1)^3+\ell^2(\ell+1)^2-\ell(\ell+1)-1\,, \tag{7}$$

$$J_2=\ell^2(\ell+1)^2\left[9+14\ell(\ell+1)+9\ell^2(\ell+1)^2\right]\,. \tag{8}$$

In the monopolar case (i.e. $\ell=0$), it takes the simple value $\mu_+=\frac{1}{2}r_H^{-1}$. This allows one to easily understand the general behavior of the potential. Let us consider a particle with a given mass μ_1 and a black hole with a horizon radius r_1. The mass of the particle may be smaller than $1/2r_1$. In this case, the local barrier and the potential well do exist for all the values of the orbital quantum number, and particles can be potentially trapped with any angular momentum. On the other hand, if μ_1 is greater than $1/2r_1$, then the ℓ-domain has to be divided into two subclasses. A critical value of the orbital quantum number, denoted ℓ_1, can then be defined by $\mu_+(\ell_1)<\mu<\mu_+(\ell_1+1)$. For all the partial waves with an orbital quantum number smaller or equal to this critical value, the potential appears as a monotonically increasing function of r from $V_\ell(r_1)=0$ to $V_\ell(+\infty)=\mu_1$. However, all the partial waves with $\ell>\ell_1$ will face the local barrier as well as the well potential.

The detailed shape of the potential is also determined by another critical mass, hereafter called $\mu_-(\ell)$, which defines the relative height of the potential barrier close to the horizon when compared with the mass of the particle. If the mass of the particle is higher than the barrier, there is no more a turning point for the system. The mass is the highest value of the potential if the equation $V_\ell^2(r)=\mu^2$ has no root above r_H. The cubic form

$$r^3-\frac{\ell(\ell+1)}{r_H\mu^2}r^2-\frac{1-\ell(\ell+1)}{\mu^2}r+\frac{r_H}{\mu^2}=0 \tag{9}$$

satisfies this criterion if $\mu>\mu_-(\ell)$, which is then given by

$$\mu_-^2=\frac{1}{27r_H^2}\left(-L_1+\sqrt{L_1^2+27L_2}\right)\,, \tag{10}$$

with

$$L_1=2\ell^3(\ell+1)^3+3\ell^2(\ell+1)^2-3\ell(\ell+1)-2\,, \tag{11}$$

$$L_2=\ell^2(\ell+1)^2\left[\ell(\ell+1)+1\right]^2\,. \tag{12}$$

In the monopolar case, it becomes $\mu_- = \frac{2}{\sqrt{27}} r_H^{-1}$. Table 1 provides the values of the critical masses in units of r_H^{-1}.

The potential is always zero at $r = r_H$ and tends to μ for $r \to \infty$.

(i) If $\mu < \mu_-(\ell)$, the potential reaches a maximum higher than μ and then reaches a minimum; if

(ii) $\mu = \mu_-(\ell)$, the maximum is exactly equal to μ and a minimum also appears; if

(iii) $\mu_-(\ell) < \mu < \mu_+(\ell)$ the potential reaches a maximum lower than μ and still admits a minimum, whereas if

(iv) $\mu \geq \mu_+(\ell)$ the potential is a monotonically increasing function of r.

This behavior is illustrated for $\ell = 0$ on Fig. 2 for masses corresponding to those four specific cases. As a direct consequence of the wave description of particles in quantum mechanics, it can be seen that bound states – due to the local minimum – can appear at the monopolar order, with *no classical equivalent*. Although particles can of course be classically trapped around a black hole, no state without angular momentum can be found if the quantum behavior is not taken into account. Just as in classical mechanics, it is the non-vanishing mass that leads to the trapping (even at the quantum level), but with specific quantum features, lying in the quantization of the angular momentum, and furthermore allowing for trapping even without any angular momentum. Furthermore, whatever the mass of the particle, a bound state will appear for high enough multipolar orders so that $\mu < \mu_+(\ell)$. This makes this phenomenon of "particle trapping" quite generic. Those bound states are described by quasi-stationary quantum states that cannot reach spatial infinity but can still make a transition to the black hole by tunneling back through the gravitational barrier.

As the qualitative features can easily be understood at the monopolar order, this particular value of the quantum angular momentum is now assumed. When $\mu < \mu_+$, the
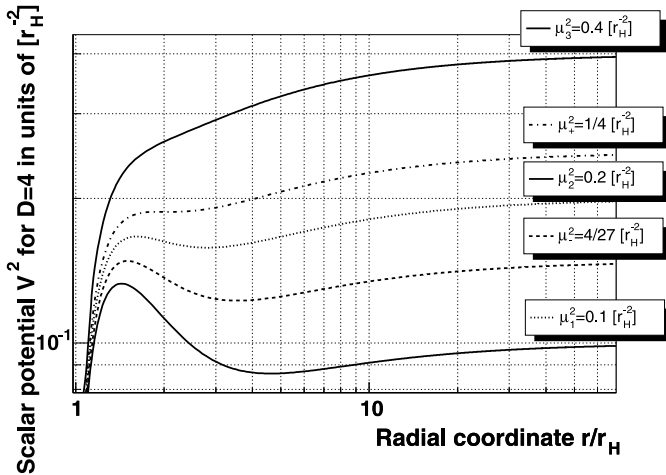
Table 1. Critical masses in units of r_H^{-1} for different angular quantum numbers

ℓ	$\mu_- \left[r_H^{-1} \right]$	$\mu_+ \left[r_H^{-1} \right]$
0	$\frac{2}{\sqrt{27}}$	$\frac{1}{2}$
1	0.794	0.931
2	1.275	1.480
3	1.768	2.046
4	2.264	2.617
5	2.761	3.191

positions of the potential barrier (r_-) and of the local minimum (r_+) can be analytically determined to be

$$r_\pm = \frac{1}{\mu} \left[\cos(\theta) \pm \sqrt{3} \sin(\theta) \right] , \qquad (13)$$

with

$$\theta = \frac{1}{3} \arctan \left[\sqrt{\left(\frac{\mu_+}{\mu} \right)^2 - 1} \right] . \qquad (14)$$

The asymptotic behavior is in agreement with the monopolar potential for a massless particle:

$$\lim_{\mu \to 0} r_+ = +\infty , \ \lim_{\mu \to 0} r_- = \frac{4}{3} r_H , \ \lim_{\mu \to \mu_+} r_\pm = 2r_H . \qquad (15)$$

The latter case, $\mu \to \mu_+$, corresponds to a saddle point at $r = 2r_H$, which represents the degeneracy of the maximum and minimum of the potential. The most important properties of the monopolar potential are summarized in the various graphs of Fig. 3. As long as the particle's mass is smaller than μ_+, the potential displays a local well and this feature may lead to the existence of quasi-stationary states localized in the well.

2.2 Complex frequency spectrum: a WKB analysis

Even when there is a well in the potential, this does not guarantee orbiting bound states to exist. To ensure the stability of those states, the local well has to be deep enough, because of the zero-point energy associated with quantum systems. Under the reasonable assumption that the shape of the potential is well approximated by a second order expression, the dynamics is similar to an harmonic oscillator with a frequency $\tilde{\omega}$ given by the curvature of the potential around its minimum:

$$\tilde{\omega} = \sqrt{d^2 V^2 / dr_\star^2 |_{r_+}} .$$

This curvature must be evaluated as a function of the tortoise coordinate, because this is the coordinate system in which the radial part of the Klein–Gordon equation is of the Schrödinger type. The zero-point energy is simply given by $\tilde{\omega}_0 = \frac{\tilde{\omega}}{2}$. The ratios of this approximated computation to the mass of the particle and to the maximum of the potential are plotted on Fig. 4. Each time a minimum

Fig. 2. Squared monopolar potential for five particle masses: (i) $\mu^2 = 0.1 r_H^{-2}$ corresponding to $\mu < \mu_-(0)$, (ii) $\mu = \mu_-(0)$, (iii) $\mu^2 = 0.2 r_H^{-2}$ corresponding to $\mu_-(0) < \mu < \mu_+(0)$, (iv) $\mu = \mu_+(0)$ and (v) $\mu^2 = 0.4 r_H^{-2}$ corresponding to $\mu > \mu_+(0)$
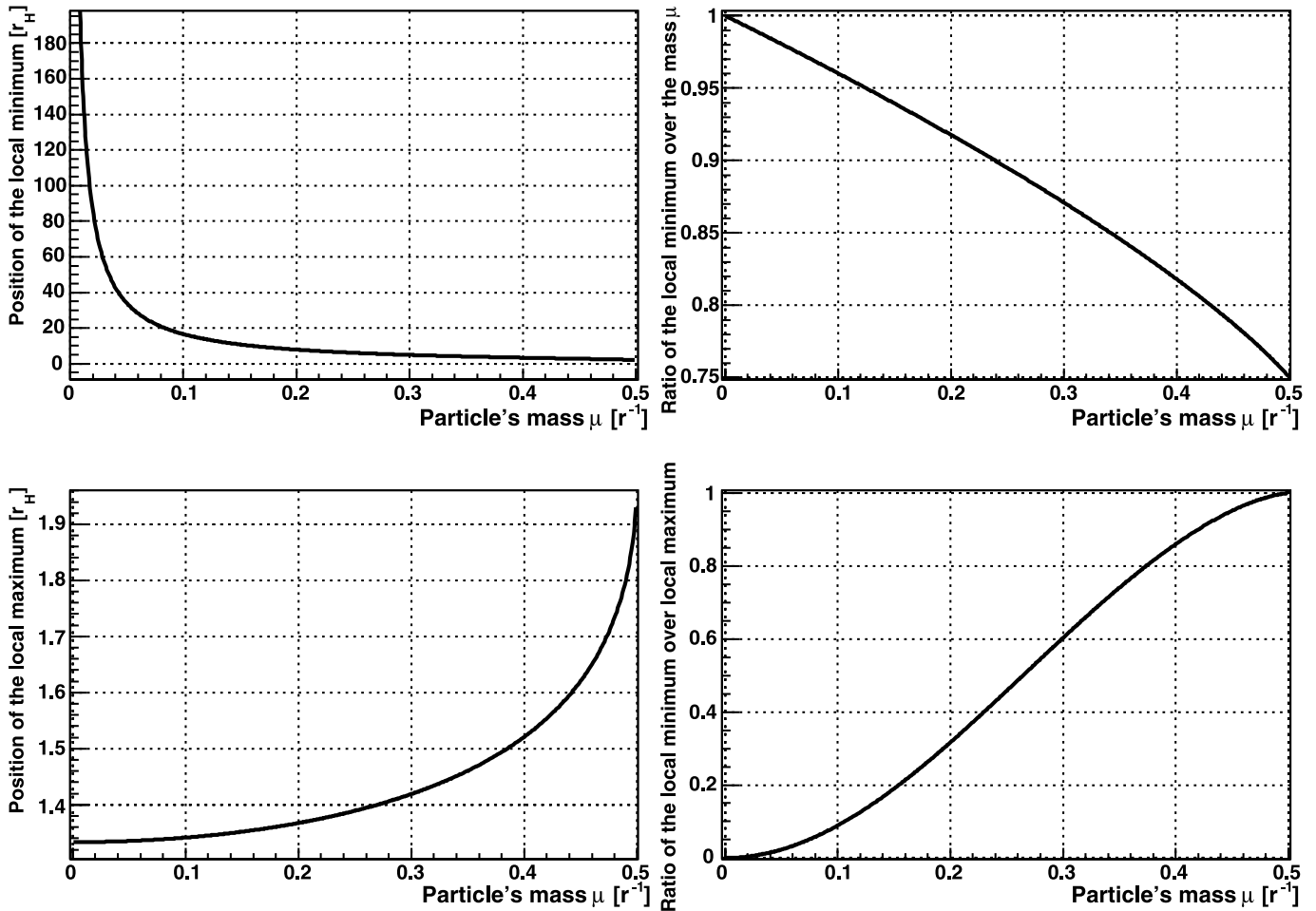
Fig. 3. *Upper left:* position of the local minimum of the potential $V_{\min}$, in units of r_H, as a function of the mass of the particle. *Upper right:* ratio of the local minimum over the mass of the particle, $V_{\min}/\mu$, as a function of the mass of the particle. *Lower left:* position of the local maximum of the potential $V_{\max}$, in units of r_H, as a function of the mass of the particle. *Upper right:* ratio of the local minimum over the local maximum, $V_{\min}/V_{\max}$, as a function of the mass of the particle

does appear, the zero-point energy remains smaller than the mass and the gravitational potential barrier, allowing bound states to exist.

Because the left part of the potential well is not an infinite barrier, the orbiting bound states are describes by quasi-stationary states associated with resonances in the density of states. Those resonances are characterized by their complex frequencies, the real part corresponding to the energy position and the imaginary part to the bandwidth. The spectrum of complex frequencies can be determined at the WKB order using the techniques developed in [9]. The spectrum will be infinite if $\mu < \mu_-$ and finite if $\mu_- < \mu < \mu_+$. The Bohr–Sommerfeld rule, whose validity in a relativistic framework was established in [9], reads (for $\forall\, n \in \mathbb{N}$)

$$\int_{r_1(\omega)}^{r_2(\omega)} \sqrt{\omega^2 - V^2(r)}\,\frac{\mathrm{d}r}{h(r)} = \left(n + \frac{1}{2}\right)\pi\,,$$

the highest frequency allowed for a bound state being μ for $\mu < \mu_-$ and $V(r_-)$ for $\mu > \mu_-$. In the latter case, the left-hand side integral is clearly finished and there exist $n_{\max}$

states. If $\mu < \mu_-$, the upper bound of the integral is infinite when $\omega = \mu$ and, the function to be integrated being proportional to $r^{-1/2}$ near $+\infty$, the spectrum is expected to be infinite. With the appropriate change of variables in the cubic equation giving the turning points, it can be shown that the normal frequency spectrum of the resonances depends only on μr_H and can be written as

$$\{\omega_n\}_{n \in \mathbb{N}} = \left\{ \frac{f_n(\mu r_H)}{r_H} \right\}_{n \in \mathbb{N}}.$$

Table 2 gives some normal frequencies and the associated bandwidths, as numerically obtained at the semi-classical order, following [10] to evaluate the tunnel probability. The quantity N_{eq} in this table will be explained in the next section.

2.3 Qualitative features of the bound states and comparison with quasi-normal modes

Before investigating the consequences of bound states for Hawking radiation, some qualitative features of those
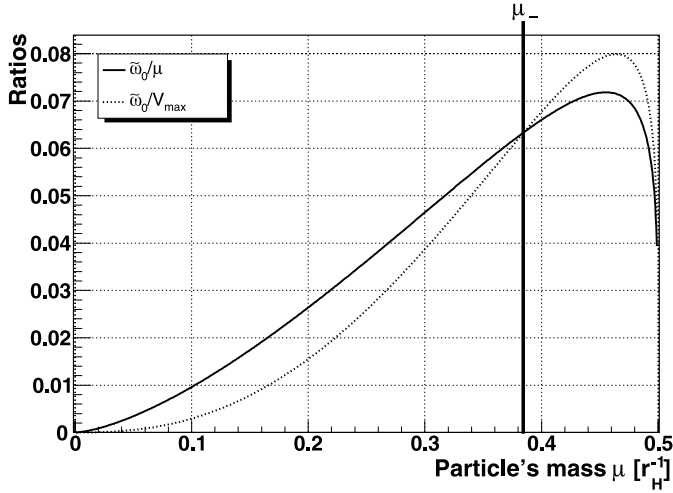
Fig. 4. Ratio of the zero-point energy $\tilde{\omega}_0$ and the mass μ and ratio of $\tilde{\omega}_0$ and the maximum of the potential $V_{\max}$, both as a function of the mass of the particle in units of r_H^{-1}

states, related to QNMs, and the existence of a halo of trapped particles around black holes, are briefly discussed in this section.

As underlined in [4], the computations of bound states and QNMs are very similar. The latter are given by the *pure outgoing* boundary conditions [6], while the former require evanescent waves at spatial infinity and ingoing modes at the black hole event horizon. However, there are no other fundamental physical links between QNMs and bound states. First of all, quasi-normal modes are related with the energy carried out by perturbations of

black holes, whereas bound states correspond to quantum states that cannot escape from the gravitational attraction. In addition [6], the mass μ of the field has to be smaller than $\mu_-(\ell)$ for QNMs to exist at the ℓth multipolar order. Moreover, because quasi-normal modes correspond to resonances near the peak of the potential, their energies have to be greater than the mass of the field. Those characteristics are direct consequences of the *pure outgoing* boundary conditions. The situation is fundamentally different for orbiting bound states. The condition on μ is less restrictive: μ has to be smaller than $\mu_+(\ell) > \mu_-(\ell)$ for orbiting bound states to exist at the ℓth multipolar order. Furthermore, the energy of those states is lower than the mass of the particle, due to the gravitational binding energy.

In addition, as long as $\mu < \mu+(0)$, bound states exist for $\ell = 0$ and a spherical halo of quanta "orbiting" the black hole can be expected. If the mass is between $\mu_+(\ell-1)$ and $\mu_+(\ell)$, bound states will exhibit an angular distribution dominated by the lowest multipolar order allowing for a minimum in the potential, that is with a distribution roughly given by $Y_m^\ell(\theta, \varphi)$. Clearly, the mass of the field has to be close to the critical masses $\mu_\pm$ for the orbiting bound states to have a substantial influence. In particular, if $\mu \ll \mu_+(0)$, the local well is so tiny at any multipolar order that particles can be treated as massless. So as to fix the orders of magnitude, Table 3 gives the masses and temperatures black holes should have so that the effects studied in this article become important for some *standard model* particles. Although they are not spinless – therefore requiring one to investigate the master equation for fermions and gauge bosons – the main qualitative features can safely be inferred from the scalar case.

Table 2. First and second rows below the integer n: spectrum of normal frequencies ω and bandwidths Γ evaluated at the WKB order in units of r_H^{-1}. Third row: number of trapped particles $N_{\rm eq}$ in the different energy levels once the equilibrium regime is reached (see the text). Three different masses are considered: $\mu < \mu_-$, $\mu = \mu_-$ and $\mu > \mu_-$

| | $\mu = 0.25 \times \mu_+$ | | | | |
n	0	1	2	3	4
ωr_H	1.24×10^{-1}	1.25×10^{-1}	1.25×10^{-1}	1.25×10^{-1}	1.25×10^{-1}
Γr_H	1.49×10^{-2}	1.49×10^{-2}	1.50×10^{-2}	1.50×10^{-2}	1.50×10^{-2}
$N_{\rm eq} r_H^{-1}$	2.15	2.09	2.09	2.09	2.09
	$\mu = \mu_-$				
n	0	1	2	3	4
ωr_H	3.75×10^{-1}	3.83×10^{-1}	3.84×10^{-1}	3.84×10^{-1}	3.85×10^{-1}
Γr_H	1.68×10^{-1}	1.87×10^{-1}	1.90×10^{-1}	1.91×10^{-1}	1.92×10^{-1}
$N_{\rm eq} r_H^{-1}$	0.024	0.021	0.021	0.021	0.020
	$\mu = 0.8 \times \mu_+$				
n	0	1	2	3	4
ωr_H	3.88×10^{-1}	–	–	–	–
Γr_H	1.91×10^{-1}	–	–	–	–
$N_{\rm eq} r_H^{-1}$	0.019	–	–	–	–

Table 3. Masses and temperatures expected for a black hole to have the critical masses $\mu_\pm$ close to the masses of some *standard model* particles

particle (mass)	$\mu = \mu_-$ for $\ell = 0$		$\mu = \mu_+$ for $\ell = 0$	
	M_{BH} [kg]	T_H [MeV]	M_{BH} [kg]	T_H [MeV]
electron (511 keV)	9×10^{13}	0.1	1.2×10^{14}	0.08
muon (105 MeV)	5×10^{11}	21.7	6×10^{11}	16.7
charm ($\simeq 1.3$ GeV)	4×10^{10}	248	5×10^{10}	190
top (171 GeV)	2.5×10^8	36×10^3	3.7×10^8	28×10^3
W boson (80 GeV)	6×10^8	16×10^3	8×10^8	12×10^3

Most *very* massive particles (like the top quark or W boson) are unstable and will decay before reaching infinity or creating a substantial halo around the hole. This point should, however, not prevent us from considering bound states associated with lighter stable particles, as the relevant parameter for the bound states to exist is not the mass of the field in itself, but the hierarchy between this mass and the mass of the hole. As far as the field is not strictly massless, there will be a black hole mass range where μ becomes close to μ_+ and μ_-, making the trapping effective.

An important issue to address is related to the time stability of those bound states. By integrating the Hawking instantaneous energy spectrum and summing over all the degrees of freedom of the standard model of particle physics, it is easy to show that the mean time between the emission of two quanta is, in Planck units, $\Delta t \approx 100M$. If we consider, e.g., electrons emitted by a black hole such that $\mu \approx \mu_-$, this leads to $\Delta t \approx 10^{-20}$ s; this remains tiny when compared to the time-scale of the black hole evolution. In other words, as the energy carried out from the hole by each emitted particle ($E \approx T = 1/(8\pi M)$) is much smaller than the mass of the hole, many quanta can be emitted and trapped before the structure of the potential will have substantially changed. This is, of course, not true anymore when $T \sim M$, that is to say in the Planck regime in which the semi-classical approximation breaks down anyway.

3 Consequences for the Hawking radiation

3.1 Trapped particles

The existence of bound states will play an important role in the Hawking evaporation mechanism which was initially described in [7] without taking into account this phenomenon.

First, some low-energy particles will be trapped by the potential well. They will not reach infinity and the spectrum will be modified in a way quite similar to what could happen due to a QCD halo [8]. When the black hole evaporates, new bound states will appear each time the temperature becomes of the same order than the critical masses

$\mu_\pm$ associated with existing particles. At the first level of approximation, the number of particles within the well per unit of time and energy, dN/dt, at a given energy is given by $F_{\mathrm{in}} - F_{\mathrm{out}}$ with $F_{\mathrm{in}} = \omega/[\tau(e^{\omega/T} \pm 1)]$ representing the ingoing one due to the Hawking evaporation, and $F_{\mathrm{out}} = N/\tau$ the outgoing one. The energy-dependent time constant $\tau = 1/\Gamma$ simply corresponds to the lifetime of the bound state. This simple model for the number of particles trapped in a local well is realistic only in the case of heavy black holes which can be considered as stationary (the small amount of energy carried out by emitted particles being much smaller that the mass of the black hole). With N_0 the initial amount of trapped particles, the time evolution is simply given by

$$N(\omega, t) = N_0(\omega)e^{-t/\tau} + \frac{1}{\omega \left(e^{-\omega/T_H} - 1\right)} \left(1 - e^{-t/\tau}\right), \tag{16}$$

which can be clearly understood as competition between particles "leaking" from the well to the hole and particles "filling" the well because of the Hawking radiation. Quickly the number of trapped particles reaches an equilibrium regime with

$$N_{\mathrm{eq}} \simeq \frac{1}{\omega \left(e^{-\omega/T_H} - 1\right)}.$$

It is worth noticing that once the equilibrium regime is reached, the number of trapped particles does not depend on τ but only on the energy and on the temperature of the black hole. This behavior is due to the fact that the probability to cross the potential barrier is the same for incoming and outgoing particles. As a consequence, the equilibrium regime, given by the ratio of the number of particles scattering off the barrier from the left and the number of particles scattering off the barrier from the right, does not depend on the lifetime of the bound states.

It is important to compare the characteristic time to reach this regime with the characteristic evolution time of the black hole. For monopolar bound states, which are dominant, and for particles with masses below μ_-, the lifetime ranges between $10M$ and $100M$. This time-scale is

of the same order as the typical time-scale between two successive emissions of a particle, which, as already mentioned in this article, is much smaller than the evolution time-scale for the black hole itself. This makes meaningful our hypothesis of *non-evolutionary black holes*: as long as heavy black holes are considered, enough particles are emitted to reach the equilibrium regime without any substantial modifications of the properties of the black hole. The expected number of trapped particles when the equilibrium regime is reached is also given in Table 2 in units of r_H^{-1}, per unit of energy and time. As can be seen from this

table, the mean number of particles decreases as the mass of the particle increases, since higher energy bound states are involved.

3.2 Greybody factors and radiation spectra

The mass of the particle will also drastically modify the greybody factors that account for the non-trivial part (gravitational barrier and centrifugal potential) of the couplings between quantum fields and evaporating black holes. The greybody factors (whose detailed study began with [11,12] followed by [13–15]) have recently been computed in quite a lot of interesting situations: extra dimensions [16], de Sitter spacetime [17], rotating black holes [18,19], Gauss–Bonnet gravity [20,21] etc., but up to now the masses of the emitted particles have mostly been ignored (although some good estimates were obtained in [15,22]). Figure 5 displays the absorption cross section numerically computed by solving the Klein–Gordon equation to evaluate the ingoing and outgoing amplitudes of the wave function at the horizon and at spatial infinity (see, e.g., [17] for a detailed description of the method we have developed). It should be pointed out that those cross sections have been computed for particles with an energy greater than or equal to the mass. Particles with an energy smaller than the mass will face an infinitely thick potential barrier, precisely due to the mass term in the potential, and will never reach spatial infinity. It should also be noticed that, when the wavelength of the particle becomes infinite, the cross section diverges, potentially leading to an experimentally
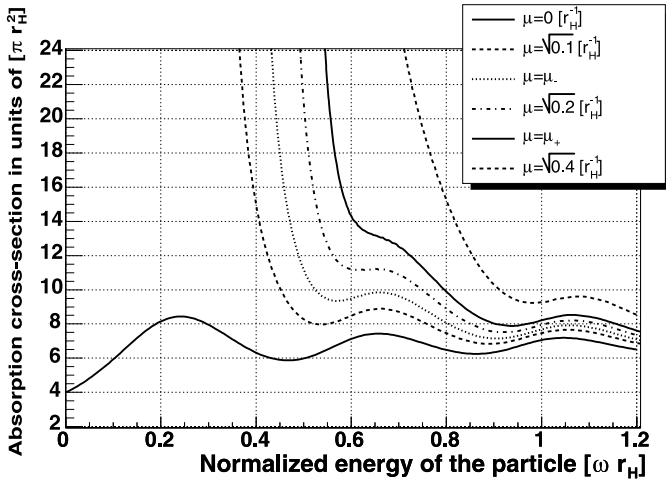
Fig. 5. Absorption cross section for massive scalar particles in units of πr_H^2 as a function of the energy measured at infinity
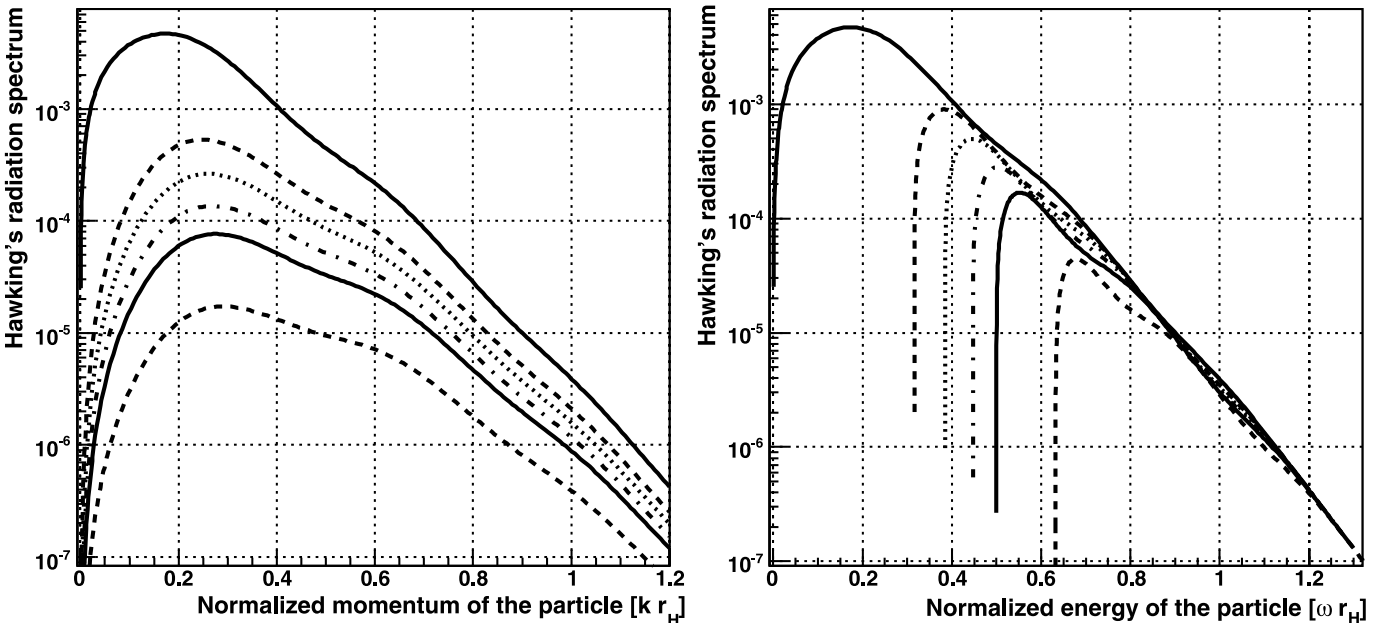
Fig. 6. Flux at infinity emitted by a black hole when taking into account the mass of the emitted particle. The different curves share the convention of Fig. 5: $\mu = 0\ [r_H^{-1}]$, $\sqrt{0.1}\ [r_H^{-1}]$, μ_-, $\sqrt{0.2}\ [r_H^{-1}]$, μ_+, $\sqrt{0.4}\ [r_H^{-1}]$ from top to bottom. *Left panel*: Hawking's radiation spectrum, $\mathrm{d}^2 N/\mathrm{d}t\,\mathrm{d}k$, as a function of the particle's momentum k. *Right panel*: Hawking's radiation spectrum, $\mathrm{d}^2 N/\mathrm{d}t\,\mathrm{d}\omega$, as a function of the energy ω of the particle

relevant enhancement of soft quanta. It can indeed be expressed as

$$\sigma_g(\omega) = \sum_\ell \frac{\pi(2\ell+1)}{k^2} |A_\ell|^2 \ ,$$

where k is the momentum (so that $\omega^2 = k^2 + \mu^2$ at spatial infinity) and $|A_\ell|^2$ is the transmission coefficient. However, the transmission coefficient remains always smaller than or equal to unity and the divergence lies in *geometrical issues*. When $\omega \to \mu$, the wave number of the particle tends to zero, whereas the transmission coefficient is non-vanishing, just because the potential barrier is not infinitely thick (the barrier precisely stops where the potential well starts and the potential tends asymptotically to μ with negative values). This leads to a k^{-2} divergence. The situation is clearly different for massless particles. In this case, the potential barrier tends asymptotically to zero with *positive values*, leading to $|A_\ell|^2 \propto k^2$ when $\omega \to 0$. This feature prevents the IR divergence from occurring for massless particles. Those results are in agreement with analytical investigations in the IR regime, $\sigma_g(k \to 0) \sim 4\pi^2(\mu r_H)^3/k^2$, as obtained following [22].

In Fig. 6, the flux at infinity emitted by a black hole is plotted when the masses of the emitted quanta are taken into account. As can be seen, this substantially modifies the usual picture both because of the intrinsic cutoff imposed by the mass and because of more subtle effects included in this analysis, like the selection induced on the allowed quantum multipolar orders of the outgoing particle. From Fig. 6, it can be seen that the radiation flux decreases for higher masses. However, in the IR limit, this tendency should change, as can be seen using the analytical limit

$$\frac{\mathrm{d}^2 N}{\mathrm{d}t\,\mathrm{d}k}(k \to 0) \sim \frac{4\pi^2(\mu r_H)^3}{\mathrm{e}^{\mu/T}-1} \qquad (17)$$

obtained from [22]. The flux is non-vanishing only if the mass of the particle is non-vanishing, enhancing the emission of ultra-soft quanta, just as for Schwarzschild–de Sitter black holes [17].

4 Conclusion

This study establishes the existence of new bound states around black holes, which, at least at the dominant monopolar order, have no classical equivalent. Although such states are known to exist in other physical systems, this opens new perspectives to investigate the detailed features of the Hawking spectrum (with possible cosmological consequences related, e.g., to the primordial power spectrum – see [23] for recent limits and [24] for a review), the intricate shape of the greybody factors and the propagation of massive quantum fields in the vicinity of a black hole. Not only could the phenomenology be revised as the spectra should be quantitatively modified but fruitful thought experiments associated with light black holes should also take into account those states. The intricate problem of backreaction should however be addressed and requires an exhaustive study in itself.

References

1. W.G. Unruh, Phys. Rev. D **14**, 870 (1976)
2. K.D. Kokkotas, B.G. Schmidt, Living Rev. Relat. **2**, 2 (1999)
3. A. Ohashi, M. Sakagami, Class. Quantum Grav. **21**, 3973 (2004)
4. S.R. Dolan, arXiv:0705.2880v1 [gr-qc]
5. P. Kanti, Int. J. Mod. Phys. A **19**, 4899 (2004)
6. L.E. Simone, C.M. Will, Class. Quantum Grav. **9**, 963 (1992)
7. S.W. Hawking, Commun. Math. Phys. **43**, 199 (1975)
8. A.F. Heckler, Phys. Rev. D **55**, 480 (1997)
9. J. Grain, A. Barrau, Nucl. Phys. B **742**, 253 (2006)
10. S. Iyer, C.M. Will, Phys. Rev. D **35**, 3621 (1987)
11. A.A. Starobinsky, Sov. Phys. JETP **37**, 28 (1973)
12. A.A. Starobinsky, S.M. Churilov, Sov. Phys. JETP **38**, 1 (1973)
13. D.N. Page, Phys. Rev. D **13**, 870 (1976)
14. D.N. Page, Phys. Rev. D **14**, 3260 (1976)
15. D.N. Page, Phys. Rev. D **16**, 2402 (1977)
16. C.M. Harris, P. Kanti, JHEP **310**, 014 (2003)
17. P. Kanti, J. Grain, A. Barrau, Phys. Rev. D **71**, 104002 (2005)
18. G. Duffy et al., JHEP **0509**, 049 (2005)
19. P. Kanti, C.M. Harris, Phys. Lett. B **633**, 106 (2006)
20. A. Barrau, J. Grain, S.O. Alexeyev, Phys. Lett. B **584**, 114 (2004)
21. J. Grain, A. Barrau, P. Kanti, Phys. Rev. D **72**, 104016 (2005)
22. W.G. Unruh, Phys. Rev. D **14**, 3251 (1976)
23. A. Barrau, N. Ponthieu, Phys. Rev. D **69**, 105021 (2004)
24. B.J. Carr, astro-ph/0511743